Journal of Mechanical, Civil and Industrial Engineering
ISSN: 2709-0809
DOI: 10.32996/jmcie
Journal Homepage: www.al-kindipublisher.com/index.php/jmcie

JMCIE
AL-KINDI CENTER FOR RESEARCH AND DEVELOPMENT

| RESEARCH ARTICLE

A Spatial Sensitivity Analysis of Flood Control Capability in the Mandalika Special Economic Zone, Central Lombok Regency, using a GIS-Based Multi-Attribute Decision Making Approach

Wanda Iqro Fatra[1]✉, Ery Setiawan[2] and I Ketut Budastra[3]
[1]Master of Engineering Student, Faculty of Engineering, University of Mataram, Mataram, Indonesia
[23]Master of Engineering Program, Faculty of Engineering, University of Mataram, Mataram, Indonesia
Corresponding Author: Author's Name, Wanda Iqro Fatra, **E-mail**: wandaiqrofatra@gmail.com

| ABSTRACT
The Mandalika Special Economic Zone (SEZ) on Lombok Island continues to develop as a national strategic area, particularly driven by rapid tourism expansion. Intensive land-cover changes, vegetation degradation, and increasing rainfall in recent years have contributed to the rise of recurrent flooding. These conditions highlight the need for a deeper assessment of flood sensitivity to support mitigation efforts and adaptive spatial planning. This study aims to evaluate the MADM scoring–weighting process, identify dominant parameters and the effects of weight variation on flood sensitivity, estimate the extent of vulnerability classes, and formulate mitigation recommendations for the area. Six parameters were used: rainfall, slope, elevation, land cover, river density, and population density. The Multi-Attribute Decision Making (MADM) method was applied using two weighting scenarios (35%–13% and 25%–15%), supported by visual verification based on morphology, color distribution, and administrative boundaries. The results indicate that medium-vulnerability zones dominate the study area, especially in transitional regions between lowlands and hilly terrain. Land cover and slope emerge as the most influential parameters, producing more stable and logical spatial patterns with weights of 0.30 and 0.25. Elevation and river density fall into the moderate-influence category, with weights of 0.15 and 0.12. Rainfall and population density show lower discrimination due to data limitations, with respective weights of 0.15 and 0.08. Land cover and slope also demonstrate the highest sensitivity, while elevation, rainfall, and river density show moderate sensitivity, and population density represents the lowest level. Medium vulnerability dominates the study area at 50.66%, followed by low vulnerability at 26.52% and high vulnerability at 22.83%. To reduce flood risk, government authorities and area managers should strengthen land-cover rehabilitation, improve spatial-planning regulations, reorganize river networks to enhance flood-control capacity, and manage population density through zoning and development monitoring.

| KEYWORDS

Flood Vulnerability, Spatial Sensitivity, Multi-Attribute Decision Making (MADM), Mandalika SEZ

| ARTICLE INFORMATION

ACCEPTED: 02 December 2025 **PUBLISHED:** 24 December 2025 **DOI:** 10.32996/jmcie.2025.6.5.7

1. Introduction

The Mandalika Special Economic Zone (SEZ), located on Lombok Island, Indonesia, has undergone rapid development following its designation as a national strategic priority area and tourism hub. This accelerated expansion has been accompanied by substantial land-cover modifications, vegetation degradation, and increasing rainfall intensity, all of which have contributed to recurrent flooding in recent years. Significant flood events recorded in 2021 and 2022 revealed the growing vulnerability of the region's hydrological systems, particularly within watersheds intersecting key tourism and residential zones. These incidents not only disrupted community mobility and damaged infrastructure but also highlighted critical gaps in spatial planning and environmental management.

Effective flood control in Mandalika requires a comprehensive understanding of the spatial factors influencing flood sensitivity, especially given the area's complex topography, evolving land-use patterns, and dense network of small to medium-sized watersheds. Previous assessments in similar developing regions often focused on single-parameter analyses, limiting their ability to capture the multidimensional nature of flood vulnerability. In contrast, Mandalika demands a more integrative approach because its sensitivity to flooding is shaped by interactions among biophysical and anthropogenic variables, including rainfall intensity, slope gradients, elevation distribution, land-cover conditions, river-network density, and population concentration.

Advances in geospatial analytics and the increasing availability of high-resolution spatial data provide new opportunities to analyze these interacting parameters more systematically. The Multi-Attribute Decision Making (MADM) method—combined with Geographic Information Systems (GIS)—offers a robust framework for evaluating parameter weights, identifying dominant controls on flood sensitivity, and quantifying spatial variations in vulnerability levels. By assigning weights to each factor and testing alternative weighting scenarios, MADM enables a structured and transparent assessment of how each parameter contributes to overall flood sensitivity. Such an approach is crucial in Mandalika, where rapid urban development and land-use conversion require continuous adaptation of flood-mitigation strategies.

Despite the strategic significance of Mandalika SEZ, scientific studies addressing its spatial flood sensitivity remain limited. This research therefore seeks to fill this gap by evaluating the MADM scoring and weighting process, identifying dominant parameters influencing flood sensitivity, and estimating the spatial extent of vulnerability classifications. The study also provides evidence-based recommendations to strengthen flood-control capability in the area, focusing on land-cover rehabilitation, improved spatial planning regulations, river-network reorganization, and population-density management.

By integrating hydrological, geomorphological, and socio-spatial variables into a single analytical framework, this study contributes to the development of more adaptive, data-driven flood-management strategies for rapidly growing economic zones in tropical regions.

2. Literature Review

Flood control capacity refers to the ability of a region to reduce, retain, and convey rainfall runoff in order to prevent inundation and environmental damage (BNPB, 2012). According to Suripin (2004), flood control is not limited to physical interventions through infrastructure development, but also involves environmental factors, land use planning, and social systems that influence the hydrological balance of a watershed. Flood control capacity can be understood as the result of interactions between biophysical conditions—such as slope, soil characteristics, and vegetation—and engineered systems, including drainage networks, levees, retention basins, and urban spatial planning. The better the condition of the natural environment and supporting infrastructure, the higher the flood control capacity of a given area. Based on the Regulation of the Ministry of Public Works and Housing (Permen PUPR) No. 04/PRT/M/2015 concerning the Criteria and Delineation of Flood-Prone Areas, several key components influence flood control capacity, as outlined below:

Physical Land Conditions

Physical land conditions include slope gradient, elevation, soil type, and land cover, all of which determine infiltration capacity and surface runoff generation (Suripin, 2004). Areas with dense vegetation cover and highly permeable soils generally exhibit better flood control capacity.

Rainfall and Hydrological Conditions: Rainfall intensity and duration are directly related to runoff volume. Higher rainfall increases hydrological pressure on both natural and artificial drainage systems (Asdak, 2010).

Flood Control Infrastructure Conditions: This component includes drainage networks, dams, detention ponds, retention basins, and urban drainage systems. Well-maintained infrastructure enhances storage capacity and accelerates surface water conveyance, thereby reducing flood risk (PUPR, 2018).

Land Use and Spatial Planning: The conversion of vegetated land into built-up or impervious surfaces significantly increases surface runoff. Effective spatial planning and land use control play a critical role in maintaining groundwater balance and flood mitigation (Fauzi et al., 2021).

Social and Institutional Conditions: Community awareness, local government capacity, and inter-agency coordination are essential elements of sustainable flood control management (BNPB, 2021).

In general, flood control capacity analysis can be conducted using a quantitative and spatial approach through a Multi-Attribute Decision Making (MADM) method integrated with a Geographic Information System (GIS). According to Malczewski (1999) and Chen and Yu (2018), the MADM–GIS approach enables the integration of multiple environmental parameters into a single, comprehensive model that produces a spatial index of flood control capacity. This method utilizes thematic maps such as rainfall, slope, soil type, land cover, population density, and flood control infrastructure. Each parameter is assigned a weight and a score based on its relative influence on flood control capacity. The weighted overlay process generates a Flood Control Potential Index, which can be classified into very high, high, moderate, low, and very low categories.

Sensitivity analysis is applied to evaluate the stability of the model with respect to variations in parameter weights. According to Saltelli et al. (2000), sensitivity analysis is essential to ensure that the final results are not overly dependent on a single dominant parameter, such as rainfall or land cover. In the context of the KEK Mandalika study, different weighting scenarios (e.g., 35%–13% and 25%–15%) were implemented to examine the effects of changes in parameter dominance on the spatial distribution of flood control capacity. If the resulting classified maps show no significant differences between weighting scenarios, the model is considered stable and robust against weighting uncertainty.

3. Methodology

3.1 Flood Events in the Mandalika Special Economic Zone

According to data from the Ministry of Public Works and Housing, Directorate of Water Resources, River Basin Authority of Nusa Tenggara I, the Mandalika Special Economic Zone (SEZ) has experienced several significant flood events, namely on 30 January 2021, 22 March 2022, and 23 December 2022. Flood event reports from the River Basin Authority of Nusa Tenggara I indicate that on 30 January 2021, flooding occurred along the Rangkap River in Kuta Village, Pujut District, Central Lombok Regency. High rainfall reaching 140.6 mm caused inundation of the river channel, agricultural fields, roads, and approximately 500 residential houses, accompanied by mud deposition. This condition was exacerbated by solid waste accumulation along major roads and drainage channels within the Mandalika SEZ. In addition, deforestation associated with maize cultivation triggered landslides, leading to blockage of drainage channels and subsequent flooding in residential areas.

On 22 March 2022, flooding occurred along the Tebeo River within the Tebelo Watershed, Kuta Village, Pujut District, with recorded rainfall of 54.32 mm based on the Rambitan ARR station and 30 mm according to the Pujut AWS station (BMKG). This flood event disrupted approximately 700 m of village roads, damaged a bridge connecting several hamlets, and inundated residential areas across six hamlets in Kuta Village.

Persistent high rainfall resulted in river narrowing by approximately 3–4 m due to sedimentation processes and the confluence of the Merendeng and Baturiti Rivers within the Tebelo Watershed. These conditions contributed to flooding on 23 December 2022 along the Ngolang and Soker Rivers, with rainfall intensities of 80.26 mm at the Mandalika ARR station and 81.70 mm at the Rembitan ARR station. The main road in front of the Mandalika Circuit was inundated along a 1.5 km stretch, causing flooding in Kuta Village with water depths reaching up to 1 m at several locations. Table 4 presents the input parameters used for the flood control capacity analysis in the Mandalika SEZ.

Table 1: Input Parameters for Flood Control Capacity Analysis in the Mandalika Special Economic Zone

Number	Parameter	Data Source	Format / Data Type	Unit	Deskripsi & Penggunaan
1	Rainfall	BBWS NT I	Rasters	mm/year	Represents the average annual rainfall intensity influencing runoff volume and hydrological pressure.
2	Slope	DEMNAS (BIG, 2023)	Rasters	%	Derived from the digital elevation model using the slope function in ArcGIS to indicate surface flow velocity potential.
3	Land Cover / Land Use	Sentinel-2 Imagery (ESA, 2024)	Rasters	Category	Describes land cover types (vegetation, settlements, paddy fields, etc.) affecting runoff generation and infiltration capacity.
4	Distance to River / Main Drainage	DEMNAS (BIG, 2023)	Rasters	meter	Calculated using Euclidean Distance to determine proximity to major flow paths and drainage channels.

Number	Parameter	Data Source	Format / Data Type	Unit	Deskripsi & Penggunaan
5	Population Density	Central Lombok Regency Statistics Agency (BPS, 2023) and Village Boundary Shapefile (BIG)	Rasters	persons/km²	Represents anthropogenic pressure on drainage systems and infiltration areas; processed as village-based zoning.
6	Elevation	DEMNAS (BIG, 2023)	Rasters	m a.s.l.	Identifies low-lying areas with higher flood potential and assesses the natural drainage capacity of the region.

3.2 Research Stages

This study adopts a quantitative descriptive approach integrating the Multi-Attribute Decision Making (MADM) method with a Geographic Information System (GIS). This approach was selected because it allows numerical processing of multiple parameters and produces spatial analyses that represent the level of flood control capacity within the study area. The MADM model was applied to determine the relative weights of each parameter, while GIS was used for spatial data processing and map generation. Subsequently, a scoring procedure was applied to all parameters included in the analysis.

Rainfall is defined as the amount of precipitation occurring in a given area over a specific period. In flood control planning, rainfall input is not based on point rainfall data but rather on the average rainfall across the entire study area. Rainfall is directly proportional to flood occurrence; higher rainfall intensities increase flood potential, whereas lower rainfall levels reduce flood risk. Slope, commonly referred to as terrain gradient, is defined as the percentage ratio between elevation difference and horizontal distance. Slope plays a significant role in flood occurrence. Steep slopes allow surface runoff to flow rapidly, thereby reducing flood potential. Conversely, gentle slopes slow down runoff, increasing the likelihood of water accumulation and flooding. Land cover quality is strongly associated with vegetation density. Vegetated areas enhance soil infiltration capacity, reduce surface runoff, and delay the concentration of flow into river channels. Consequently, the likelihood of flooding decreases compared to areas with limited or no vegetation cover.

Drainage density is defined as the total length of river channels per unit area of a watershed. High drainage density generally indicates efficient runoff conveyance, while low drainage density increases infiltration potential. However, excessive runoff combined with limited infiltration may increase flood risk. According to Linsley (1975) in Darmawan et al. (2017), watersheds with drainage density values below 0.62 km/km² tend to experience inundation, whereas values above 3.10 km/km² are commonly associated with dry conditions. Elevation represents the height of a location above mean sea level. Low-lying areas are more susceptible to flooding than higher-elevation areas. Higher elevations generally indicate lower flood risk. Population density significantly influences environmental conditions and land use change (Kuswadi, 2014). Rapid population growth often leads to land conversion from vegetated areas to built-up settlements, affecting runoff volume and flow timing. Increased surface runoff may result in downstream flooding.

This study applies a scoring and weighting method to all parameters based on their relative influence on flood occurrence. The weighted parameters were analyzed using the MADM framework integrated with GIS. During data preparation, grid size selection was carefully considered, as inappropriate grid resolution may produce misleading flood vulnerability results (Zhan et al., 2022). Flood vulnerability maps for the period 2013–2022 were subsequently compared to assess parameter sensitivity. Vulnerability classification was conducted based on environmental and social indicators. The weighting factors are presented in Table 2.7, and class intervals were determined using the following equation (Carolita, 2014 in Pratama, 2020):

$$Ki = \frac{Xt - Xr}{k} \quad \text{..... (1)}$$

where:

Ki : class interval,
Xt : maximum value,
Xr : minimum value,
K : number of desired classes.

The weighting stage was conducted using the Analytical Hierarchy Process (AHP) or other derivative methods of Multi-Attribute Decision Making (MADM) to determine priority weights among the selected parameters. In this study, two experimental

weighting scenarios were applied to evaluate parameter sensitivity, including rainfall, slope, land cover, drainage density, elevation, and population density. These six parameters were assigned different weight combinations under two scenarios, as detailed in Table 2, to assess the influence of parameter dominance on the resulting flood control capacity analysis.

Table 2: Weight Distribution of Parameters in the Spatial Sensitivity Analysis for the 35%–13% and 25%–15% Scenarios

	Sensitivity parameter	Other Contributing Parameters					Total
No	1	2	3	4	5	6	7
Weight	35%	13%	13%	13%	13%	13%	100%
Weight	25%	15%	15%	15%	15%	15%	100%

Both weighting scenarios were employed to test the stability of the model through sensitivity analysis. Sensitivity analysis using alternative weighting scenarios provides theoretical insight into the influence of dominant indicators on the vulnerability model. From a practical perspective, it also serves as a basis for policy decision-making in identifying more appropriate flood control strategies. Spatial sensitivity analysis was conducted by assigning a relatively dominant coefficient to one indicator while distributing smaller coefficients evenly among the remaining indicators.

To ensure the accuracy of spatially based flood vulnerability modeling, purely quantitative evaluation is insufficient. In a geospatial context, visual validation of model outputs is an integral component in assessing the feasibility and consistency between model predictions and actual spatial conditions in the field. Therefore, a set of visual indicators is required to guide the interpretation of model-generated maps in a systematic, logical, and objective manner. These indicators function as key benchmarks for evaluating the spatial–conceptual consistency of each scenario map. This evaluation forms part of a visual spatial sensitivity analysis approach, which has been widely applied in recent geospatial studies, particularly those integrating environmental data with Geographic Information Systems (GIS).

Through visual assessment, it is possible to determine whether the spatial distribution of color classes (e.g., green, yellow, and red) corresponds with geomorphological characteristics, land cover patterns, topography, and empirical evidence such as recorded flood locations. This visualization enables researchers to assess not only the internal validity of the model but also the interpretability and practical relevance of the resulting maps.

Accordingly, this study developed a visual indicator–based evaluation system structured into several main categories, each consisting of multiple sub-indicators representing specific spatial aspects. In general, the indicators are classified into four major groups: (1) Spatial–Conceptual Consistency Indicators, (2) Color Distribution Indicators, (3) Visual Sharpness Indicators, and (4) Visual Distortion Indicators. Each indicator group was designed to capture critical dimensions of map interpretation in flood vulnerability modeling. The visual indicators and sub-indicators used as references for visual vulnerability analysis are presented in Table 3.

Table 3: Spatial Sensitivity Evaluation Indicators

No	Visual indicator	Description
1	Spatial–Conceptual Consistency	Assesses whether the color patterns on the map are consistent with spatial concepts such as topography, elevation, upstream–downstream flow, land-use changes, infrastructure, and alignment with actual flood locations.
2	Color Distribution	Evaluates whether the distribution of green–yellow–red zones is spatially logical, has proper transitions, does not overrepresent safe areas, and displays clear zone contrasts.
3	Visual Sharpness	Assesses the clarity of spatial patterns: color consistency, the ability to distinguish between vulnerable and safe areas, appropriate heterogeneity, and alignment with actual land-use conditions.

The first indicator group, Spatial–Contextual Consistency, addresses the model's ability to represent the correspondence between vulnerability zones and key spatial features such as elevation, topography, land use, and observed flood locations. Indicators within this group evaluate spatial logic, namely whether high-vulnerability zones (red) are located in low-lying areas or densely populated settlements, and whether low-vulnerability zones (green) are situated in upland, forested, or hilly areas. This group constitutes the primary foundation of model validation, as it directly reflects geological and geographical conditions.

The second indicator group, Color Distribution, evaluates the balance and realism of the spatial distribution of low (green), moderate (yellow), and high (red) vulnerability zones across each scenario map. Indicators in this group assess dominant color consistency, the accuracy of transitional zones (yellow), and the spatial distribution of high-vulnerability areas. This evaluation is essential to ensure that no single class excessively dominates the map (e.g., the entire area classified as moderate) and to identify anomalies, such as high-vulnerability zones occurring in geomorphologically implausible locations.

The third indicator group, Visual Sharpness, assesses the model's ability to clearly distinguish between safe and vulnerable areas and evaluates whether the visualization provides sufficient contrast and interpretability. This group reflects the classification strength of the model in filtering spatial information and producing maps that are communicative and informative for both policymakers and the general public.

The fourth indicator group, Visual Distortion, is used to identify model artifacts resulting from non-spatial influences, particularly administrative boundaries. This indicator is critical because a robust model should define flood vulnerability based on environmental and geophysical conditions rather than administrative units. The appearance of block-like high-vulnerability zones covering entire villages without consideration of topography or land cover indicates invalid dependence on social or administrative data.

Each indicator was evaluated using a visual scoring system based on direct observation of model output maps across multiple scenarios and years. Scores were assigned to dominant parameters under two primary weighting scenarios (35:13 and 25:15) for the period 2017–2023. Visual assessment followed a systematic approach using predefined indicators, with scores assigned on a quantitative scale of 1–5, where the highest score (5) represents the strongest spatial consistency and map quality, and the lowest score (1) indicates the opposite.

The primary purpose of developing these visual indicators was not merely to support subjective evaluation, but to bridge data-driven modeling and applied spatial interpretation. Furthermore, these indicators assisted in determining the final parameter weights by assessing how effectively each parameter contributed to producing logical and valid vulnerability patterns.

4. Results/Findings

4.1 Parameter

Drainage density represents the number and total length of river channels per unit area. Similar to slope, drainage density was derived from DEM data, as illustrated in Figure 4.3. Areas with numerous tributaries or dense natural drainage networks typically exhibit more complex hydrological flow systems; however, they also face a higher flood risk when channel capacity is insufficient or when blockages occur.

This parameter was classified based on river morphology and branching intensity. A higher degree of branching indicates greater drainage density, which accelerates the accumulation and concentration of surface runoff toward outlet points. Consequently, peak runoff (flood discharge) occurs more rapidly and with greater magnitude. Therefore, drainage density must be analyzed in conjunction with rainfall and land-cover parameters.

Scoring was assigned based on river length per square kilometer, ranging from 1 (very low) to 5 (very high). In the Mandalika Special Economic Zone (KEK Mandalika), the drainage network is relatively dense, particularly in the central and southeastern areas. This spatial pattern remains relatively stable over the study period. Figure 1 shows the scoring results of the drainage density parameter.

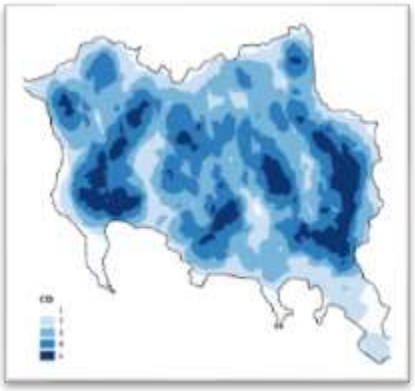

Figure 1: River density parameter scoring map

Figure 1 above indicates that the river density level in the study area is predominantly very high. This condition is reflected by the extensive distribution of dark blue areas representing a score of 5, which is relatively balanced with areas assigned a score of 4. Areas with a score of 3 are evenly distributed across the region, followed by limited areas classified as score 2 and only a very small proportion categorized as score 1. This spatial pattern suggests that the spatial vulnerability analysis in the study area is likely to result in a relatively extensive distribution of flood-prone zones.

Slope, commonly referred to as terrain gradient, is defined as the percentage ratio between elevation change and horizontal distance. In this study, slope was analyzed using the national digital elevation model (DEMNAS). Slope plays a critical role in controlling surface runoff velocity. Steep slopes allow water to flow rapidly downstream, thereby reducing the potential for water accumulation, whereas gentle slopes significantly increase the likelihood of ponding and inundation. In the study area, slope distribution varies considerably between the western and eastern parts, where upstream regions exhibit steep topography while downstream areas are predominantly flat. Slope classes were assigned scores ranging from 1 for steep slopes (>45%) to 5 for flat slopes (0–8%). Although slope is a relatively static parameter, it remains highly relevant in flood vulnerability assessment, as it governs flow pathways and floodwater accumulation, particularly when combined with land cover conditions. Based on Figure 2, the study area is strongly dominated by slopes classified as score 5. This dominance indicates that most of the area consists of flat terrain with slope gradients of 0–8%, which substantially increases flood susceptibility. Consequently, this condition suggests that the spatial flood vulnerability analysis is likely to result in a relatively extensive distribution of vulnerable areas.

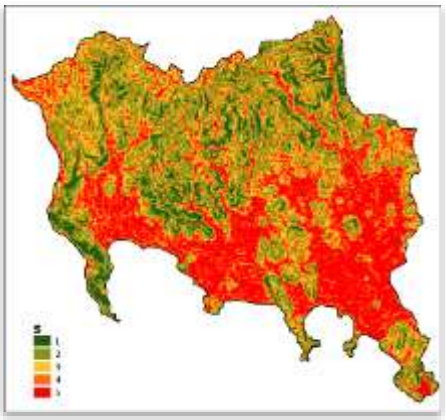

Figure 2: Slope parameter scoring map

Elevation is a critical factor in understanding surface runoff direction and accumulation patterns. Similar to the slope and river density parameters, elevation was derived from digital elevation model (DEM) data, as illustrated in Figure 4.3. Low-lying areas, particularly coastal plains, are highly susceptible to flooding, especially when located near river downstream sections or estuarine zones. In contrast, elevated or hilly regions tend to be less vulnerable to flooding, although they may still present hazards related to landslides or rapid runoff.

Elevation classes were assigned scores ranging from 1 for areas higher than 200 m above sea level to 5 for areas lower than 10 m above sea level. From a spatial perspective, elevation plays a crucial role in shaping natural catchment zones and controlling water convergence. The elevation scoring therefore assists in identifying potential stagnation zones and areas prone to surface water accumulation, which are key indicators of flood vulnerability.

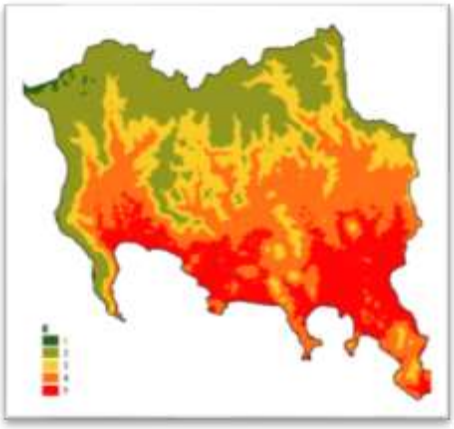

Figure 3: Elevation parameter scoring map

Based on Figure 3, the elevation parameter exhibits a stable scoring pattern due to its static nature. However, areas located at low elevations consistently receive high scores (4–5), particularly in coastal zones and downstream river plains. In the final modeling results, these zones become priority areas for mitigation efforts, as their topographic characteristics make them highly susceptible to tidal flooding and runoff contributions from upstream regions.

Areas with a score of 2 are predominantly distributed across the central part of the study area, while areas assigned a score of 1 are very limited and mainly located in upstream regions. This spatial pattern indicates that the flood vulnerability analysis is likely to produce a relatively extensive vulnerable area within the study region.

Population density represents a social parameter that influences the magnitude of flood impacts on human systems. This parameter was derived using village administrative boundaries as the primary spatial unit, with population density values assigned as attribute data, as illustrated in Figure 4. Areas with higher population densities are associated with greater potential losses, including casualties, economic damage, and increased evacuation requirements. Although population density does not directly influence flood occurrence, it plays a critical role in flood vulnerability modeling. The scoring scheme ranges from 1 (very low population density) to 5 (very high population density).

Population density is closely linked to land use characteristics. High population concentrations tend to drive land-use transformation, such as the conversion of forested areas into residential settlements. As residential areas expand, open spaces that function as infiltration zones decrease, thereby increasing surface runoff and the likelihood of flooding. Based on land-use classification, residential areas are considered among the most flood-prone zones. Population density values were calculated by dividing the total population by the area of each administrative unit.

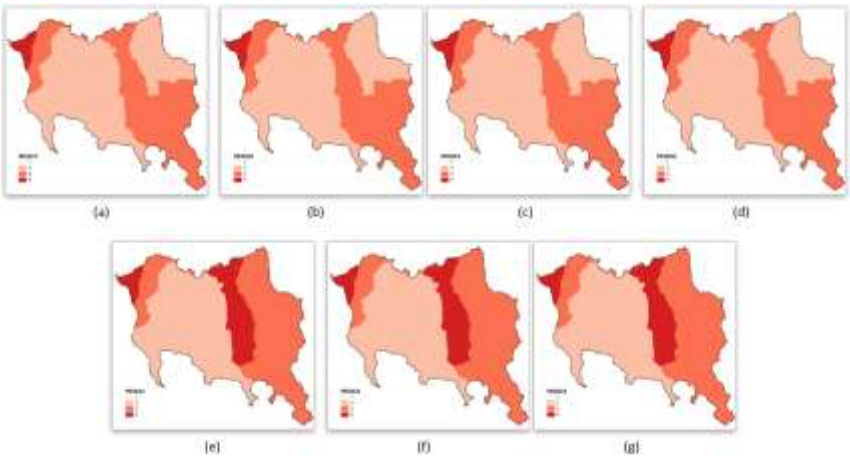

Figure 4: Elevation parameter scoring map for 2017-2013 (a-g)

Figure 4 illustrates a gradual increase in population density from 2017 to 2020 and from 2021 to 2023, particularly in the core tourism villages. This trend results in a consistent increase in population density scores, reflecting the rising social and economic risks associated with potential flood events. The score increase is especially evident in the eastern part of the study area.

Well-managed land cover is characterized by areas dominated by vegetation. Vegetation enhances soil infiltration capacity, thereby reducing surface runoff that contributes to river discharge and potential flooding. The land cover data used in this study were derived from a time series of Sentinel-2 imagery provided by ESRI. These data were subsequently classified, assigned values, and scored for further analysis.

Land cover plays a critical role in determining the infiltration capacity of a region. Areas dominated by vegetative cover, such as forests, shrublands, and agricultural lands, are able to reduce surface runoff due to their high soil infiltration capacity. In contrast, areas that have undergone land conversion into settlements or built-up surfaces tend to be impermeable, leading to increased surface runoff. In urban areas and tourism destinations such as the Mandalika Special Economic Zone (KEK Mandalika), land use dynamics change rapidly, thereby increasing hydrological instability. Consequently, this parameter represents a highly dynamic and crucial factor in flood vulnerability assessment. Land cover scoring was assigned from a value of 1 for natural vegetated areas to 5 for impervious surfaces.

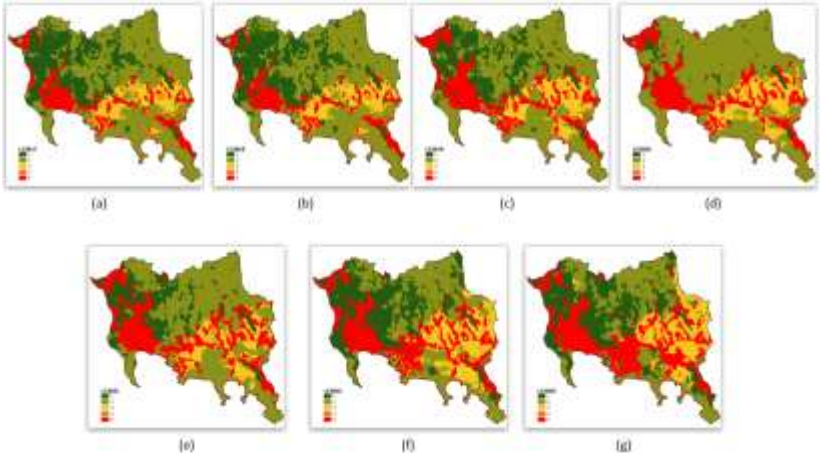

Figure 5: Land-cover parameter scoring map for 2017-2013 (a-g)

Figure 5 shows relatively stable land cover scoring results during the 2017–2019 period, in which this parameter was predominantly characterized by a score of 2. During this interval, areas of vegetative cover assigned a score of 1 were still clearly present, although they were less extensive than areas with a score of 2. Scores 3 and 5 were relatively evenly distributed, followed by a small proportion of areas classified as score 4.

In 2020, a decline in land cover quality was observed, as areas with a score of 2 became highly dominant across the study area. This was followed by a relatively balanced distribution of scores 3 and 5, with very limited areas classified as scores 1 and 4.

Land cover conditions began to improve again in 2021, marked by the re-emergence of vegetated areas with a score of 1. A more pronounced improvement in land cover quality occurred during 2022–2023, when areas with a score of 1 expanded considerably, accompanied by a balanced distribution of scores 3 and 5 and a consistently minimal extent of score 4 areas.

Rainfall represents the primary dynamic factor that directly influences flood occurrence. Higher annual rainfall results in greater surface runoff and overland flow generation, thereby increasing flood potential. Consequently, areas experiencing higher rainfall exhibit greater flood vulnerability. Rainfall scores were determined based on annual mean values, ranging from 1 for very dry areas to 5 for very wet areas. The rainfall parameter scores for the KEK Mandalika area during the 2017–2023 period is presented in Figure 6.

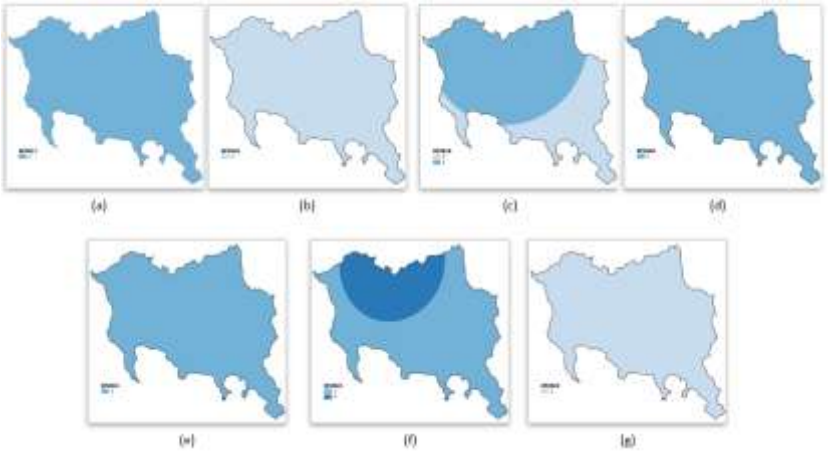

Figure 6: Rainfall parameter scoring map for 2017-2013 (a-g)

The rainfall parameter exhibits a highly fluctuating temporal pattern. The years 2018 and 2023 recorded the lowest rainfall levels, reflecting relatively dry conditions across the study area. An increase in rainfall was observed in 2019, transitioning from dry to moderately wet conditions with a relatively uniform spatial distribution. Overall, rainfall conditions were consistently classified as moderately wet during 2017, 2020, and 2021. In contrast, 2022 experienced a pronounced and extreme increase in rainfall, characterized by conditions ranging from moderately wet to wet.

4.2 Discussion

Overall, the evaluation results indicate that the land cover parameter consistently achieved the highest visual scores across all years. This finding suggests that land cover is the most effective parameter in generating flood vulnerability zone patterns that closely reflect real-world conditions, in terms of morphological consistency, color classification, and visual clarity between zones. Under this parameter, high-vulnerability zones (red) tend to occur in densely built-up areas, transitional zones (yellow) appear in open land or plantation areas, and low-vulnerability zones (green) are concentrated in forested and hilly regions, demonstrating strong spatial logic. A similar pattern is observed for the slope parameter, where high-vulnerability zones dominate flat areas near river channels, while low-vulnerability zones are consistently located in upland areas.

In contrast, parameters such as population density and river density received lower visual scores for several sub-indicators. For population density, the spatial visualization shows a strong dependence on administrative boundaries at the village or sub-district level, which reduces the spatial validity of the model. This is evidenced by the dominance of yellow or red zones forming block-like administrative patterns that do not follow topographic contours. For river density, limitations arise from the use of overly wide river buffers, resulting in hilly areas being classified as moderate to high vulnerability zones solely due to their proximity to rivers, despite being topographically less susceptible to flooding.

The elevation, slope, and river density parameters exhibit relatively stable performance, with moderate to high visual scores. Across multiple scenarios, these parameters generate clear green zones in upland areas and consistent red zones in low-lying regions. However, challenges emerge in transitional elevation zones when these parameters are not adequately balanced by supporting variables, causing yellow zones to appear less proportionally. In the case of river density, although the overall score is moderate, the spatial distribution of vulnerability remains less logical, as the map is dominated by yellow zones and extensive red buffer areas.

For rainfall and population density parameters, visual scores vary considerably depending on annual conditions. In 2022, when rainfall reached extreme levels, these parameters exhibited improved spatial performance compared to years with relatively stable rainfall, such as 2018. This suggests that these parameters are highly sensitive to extreme hydrometeorological events but are less effective in capturing fine-scale spatial differentiation under more homogeneous rainfall conditions.

The average visual scores for each parameter indicate that models dominated by primary parameters—such as land cover, slope, and elevation—tend to produce more spatially logical results and more effectively represent flood vulnerability. This finding strengthens the argument that these parameters should be assigned higher weights in the final MADM analysis. Meanwhile, supporting parameters such as rainfall, population density, and river density remain important, but their role is more complementary, serving to balance transitional zones or provide additional sensitivity within the model.

From a temporal perspective, score fluctuations highlight the importance of incorporating annual dynamics into flood vulnerability analysis. During extreme years, such as 2022, the spatial extent of high-vulnerability zones expanded considerably, and models dominated by supporting parameters became more relevant because they were able to capture anomalous conditions more effectively. In contrast, during normal or hydrologically stable years, primary parameters demonstrated much higher consistency. Therefore, a proportional integration of both parameter types is essential to produce a final model that is not only technically accurate but also adaptive to spatial and interannual climatic variability.

Overall, these findings demonstrate that visual evaluation methods provide more than supplementary validation for spatial models; they also play a critical role in guiding decision-making related to final parameter weighting. By considering the spatial visual performance of each parameter, researchers can determine optimal final weights, thereby enhancing the reliability of flood vulnerability models for spatial planning, mitigation strategies, and policy formulation.

Parameter classification is essential for distinguishing variables that exert a dominant influence on the spatial distribution of flood vulnerability from those that function primarily as modifiers or contextual adjustments related to social conditions. Accordingly, parameters were classified into two major categories: Primary Parameters and Supporting Parameters. This classification is based not only on the frequency of strong spatial influence observed in visual evaluations but also on scientific considerations regarding how each parameter interacts with flood-generating mechanisms within the study area.

Primary parameters are those that exert direct, strong, and significant influence on physical flood processes, including infiltration, surface runoff, overland flow, and water accumulation zones. These parameters exhibit high sensitivity to environmental changes and consistent spatial patterns across multiple years. Supporting parameters, in contrast, do not directly cause flooding but influence the spatial distribution of impacts, social vulnerability, or reflect the capacity of flood control systems within a given area.

This parameter classification is inherently dynamic and context-dependent. In regions characterized by poor drainage networks, river density may act as a primary parameter. However, in the context of the present study area—where open drainage systems exist alongside rapidly developing urban zones—land cover and topographic characteristics exert greater control over flood vulnerability patterns. Based on visual spatial evaluations of the six parameters and supported by temporal observations from 2017 to 2023, primary parameters demonstrate high consistency in forming spatially logical high-vulnerability (red) and low-vulnerability (green) zones. Supporting parameters primarily function to refine and complement the model, improving its adaptability to social variations and annual rainfall fluctuations.

In this study, land cover, slope, and elevation are classified as Primary Parameters. Land cover directly controls soil infiltration capacity and surface runoff generation; areas dominated by built-up surfaces exhibit low infiltration and consequently higher flood vulnerability. Similarly, slope influences flow velocity, where low-gradient areas are more prone to water accumulation and flooding. Elevation plays a critical role in determining water convergence, with low-lying areas serving as natural accumulation zones for runoff originating from upstream regions.

Population density, rainfall, and river density are categorized as Supporting Parameters. Population density does not directly cause flooding but significantly increases social risk and vulnerability when flooding occurs. This parameter is also strongly influenced by administrative boundaries, causing its spatial pattern to reflect demographic distributions rather than natural spatial processes. Rainfall, although a direct trigger of flood events, tends to exhibit relatively homogeneous spatial distribution at local scales, limiting its ability to differentiate vulnerability between adjacent areas. Consequently, rainfall is more appropriately classified as a flood-triggering factor rather than a determinant of spatial vulnerability patterns. Similarly, river density—while important for

identifying flow pathways—often produces visual anomalies in spatial modeling due to buffer zones that are disproportionate to actual topographic and land cover conditions. A summary of parameter categories and their relative sensitivity levels in flood vulnerability assessment is presented in Table 4.

Table 4: Spatial Sensitivity Classification of Flood Vulnerability Parameters

No	Indicator	Parameter Category	Sensitivity Level
1	Rainfall	Supporting	Moderate
2	Land Use / Land Cover	Primary	High
3	Population Density	Supporting	Moderate
4	Slope	Primary	High
5	Elevation	Primary	Moderate
6	River Density	Supporting	Moderate

Systematically, the primary parameters exhibit a high level of sensitivity to changes in weighting scenarios. This is evident from the significant shifts in spatial distribution when these parameters are assigned a dominant weight of 35%, compared to a lower weight of 25%. In contrast, although supporting parameters produce visible spatial color variations, their resulting patterns tend to be inconsistent with topographic conditions and the actual distribution of flood vulnerability observed in the field. Therefore, in determining the final recommended weighting scheme, primary parameters are assigned higher proportional weights due to their substantial contribution to generating a more accurate and rational flood vulnerability model, as presented in Table 5.

Table 5: Recommended weighting factor values for flood vulnerability parameters

No	Parameters	Value
1	Rainfall	0.10
2	Land cover	0.30
3	Population density	0.08
4	Slope	0.25
5	Elevation	0.15
6	Channel density	0.12

The use of data derived from different sources may result in variations in analytical outcomes and, consequently, require different weighting values. Nevertheless, the classification of parameters into primary and supporting categories, as defined in this study, remains applicable as a reference for future research. Minor adjustments to weighting values are necessary to account for differences in data quality and the specific characteristics of the watershed or study area being analyzed.

Overall, the mapping results indicate that flood vulnerability levels within the Mandalika Special Economic Zone (KEK Mandalika) range from low to high. The spatial distribution of vulnerability classes exhibits patterns that are consistent with the area's topographic conditions and land-use characteristics.

High flood vulnerability zones are predominantly distributed across the central area to the western coastal zone of KEK Mandalika, particularly around Kuta Village and its surrounding areas. These zones are characterized by dense residential land use, intensive tourism-related development activities, and relatively low elevation (<20 m above sea level). The combination of high population density, dense networks of small rivers partially obstructed by infrastructure, and reduced infiltration areas due to land-use conversion constitutes the primary factors contributing to increased surface runoff and inundation potential in this region.

Moderate vulnerability zones are mainly located in areas with gentle to moderate slopes and relatively open land-use patterns, such as shrubland and vacant land, particularly in the eastern part of KEK Mandalika. In contrast, low vulnerability zones are found in areas with relatively higher elevations and steeper slopes in the northern and northeastern parts of the study area. These conditions facilitate rapid drainage of rainfall runoff toward downstream areas, thereby reducing the likelihood of water stagnation and flooding. Figure 7 presents the flood vulnerability maps for the period 2017–2023, overlaid with flood-affected area data obtained from BNPB, providing a comprehensive depiction of the temporal and spatial dynamics of flood vulnerability in the study area.

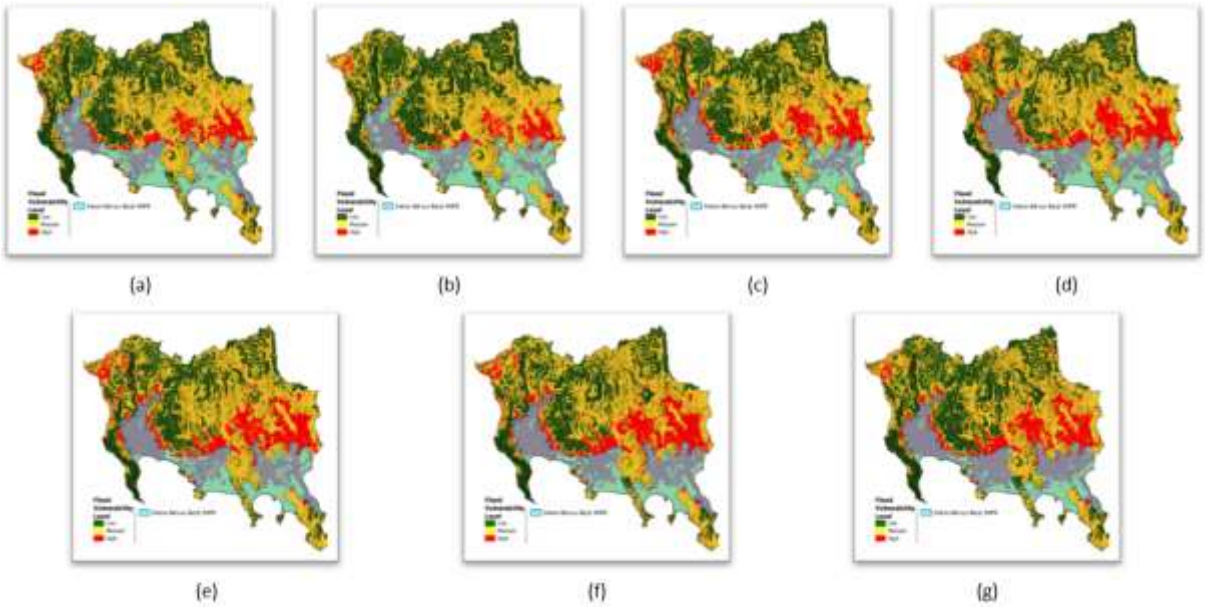

Figure 7: Overlay of BNPB Flood Vulnerability Extent with the Flood Vulnerability Analysis Results for 2017-2023 (a-g)

Figure 8 illustrates the dynamics of changes in the percentage of flood vulnerability areas during the 2017–2023 period, classified into three main categories: Low, Medium, and High vulnerability. In addition, the graph includes a BNPB reference line, which serves as a threshold for high flood vulnerability, facilitating the evaluation of the consistency between the modeling results and national disaster risk standards. This temporal analysis aims to examine how variations in physical and anthropogenic factors influence the spatial distribution of flood risk over time.

The Medium vulnerability class consistently dominates the study area throughout the observation period. This indicates that the majority of the region remains in a transitional condition—neither entirely safe from flood hazards nor categorized as highly vulnerable. Such conditions are generally associated with a combination of moderate slopes, semi-open land cover, and relatively high river density.

In contrast, the Low and High vulnerability classes exhibit more dynamic fluctuations over time. These variations reflect the sensitivity of the model to changes in parameters such as annual rainfall variability, land-cover dynamics, and increasing population density in specific areas. In this context, the presence of the BNPB reference line is particularly important, as it functions as a benchmark to assess whether the extent of high vulnerability zones remains within acceptable risk limits or exceeds established warning thresholds. Therefore, this graph serves not only as a statistical visualization but also as an evaluative tool for assessing the stability of the modeling results, the effectiveness of parameter weighting, and the long-term policy implications for sustainable flood risk management.

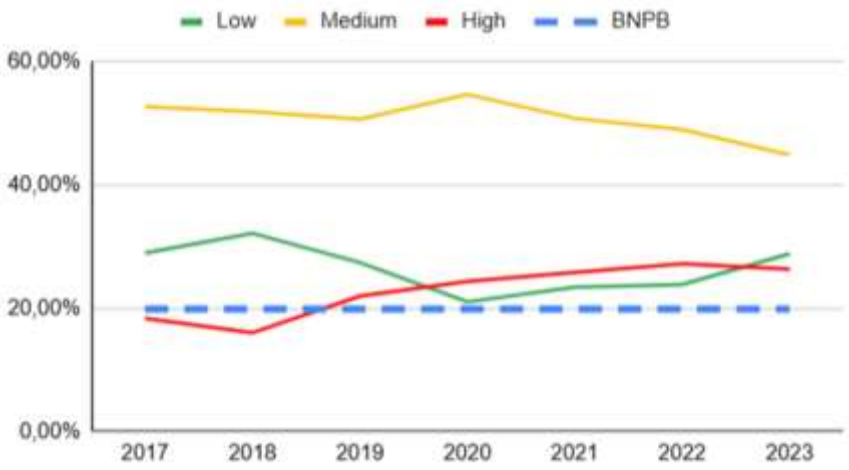

Figure 8: Comparative graph of flood vulnerability areas for 2017–2023

Based on the graph, the proportion of areas classified as medium flood vulnerability ranges between approximately 45–55% and shows a declining trend after reaching its peak in 2020. This decrease can be interpreted as the combined effect of improvements in land-cover conditions and adjustments in the weighting of dominant parameters, which resulted in a redistribution of vulnerability zones toward the Low and High classes. Nevertheless, the continued dominance of the medium vulnerability class indicates that the study area still requires considerable attention in flood risk management, particularly in zones that have the potential to escalate into higher vulnerability levels.

The Low vulnerability class exhibits a fluctuating pattern, with a decrease observed in 2020 followed by a gradual increase up to 2023. This pattern suggests a shift of certain areas toward relatively safer conditions, potentially influenced by improvements in land-cover quality or the stability of topographic factors. However, these fluctuations also imply that low-vulnerability zones remain sensitive to changes in land-use policies and development pressures.

In contrast, the High vulnerability zone demonstrates a gradual increasing trend since 2018 and has consistently remained above the BNPB reference line after 2019. This condition indicates an expansion of high-risk areas that has surpassed the national alert threshold. The increase is closely associated with the concentration of low-lying areas, coastal zones, and regions with high population density, which are physically and socially more susceptible to flood hazards.

Overall, the graph emphasizes that although some areas show improvement toward lower vulnerability classes, the expansion of high-vulnerability zones represents a critical warning signal. Therefore, mitigation strategies should prioritize land-use control, river and drainage system management, and regulation of built-up area expansion to sustainably suppress the increasing trend of flood risk.

At least three out of the six analyzed parameters can be directly intervened in flood management efforts within the study area, namely land use, river density, and population density.

Land Cover/Land Use

Rapid land-use changes driven by infrastructure development within the KEK Mandalika area have significantly reduced soil infiltration capacity and increased surface runoff. Areas that were previously dominated by open land and shrub vegetation have been converted into built-up zones with impervious surfaces, particularly around The Mandalika Circuit, hotel developments, and major access roads. As a result, rainfall is no longer optimally absorbed by the soil, leading to localized water accumulation, especially in low-elevation areas. Mitigation efforts to address land-use issues may include drainage-oriented spatial planning that follows natural flow paths, the implementation of green infrastructure such as infiltration parks and biopores, and stricter control of land-use conversion in river buffer zones and low-lying areas.

River Density

River density in the KEK Mandalika area exhibits considerable spatial variation, particularly between the northern and southern parts of the region. The southern area, which directly borders the coastline, is characterized by relatively low river density.

In contrast, the northern and central parts of the study area show higher river density, with several tributaries draining toward the Seger and Kuta coastal zones.

Overlay analysis indicates that areas with low river density tend to have lower flood control capacity. This condition occurs because surface runoff lacks adequate drainage pathways, causing water to accumulate and remain on the land surface for longer periods. Conversely, areas with higher river density generally demonstrate more effective runoff distribution, thereby reducing the potential for prolonged inundation.

Mitigation measures to address issues related to river density may include rehabilitation of natural river networks and drainage channels, control of sedimentation and solid waste within waterways, construction of connecting channels to convey runoff toward main rivers through retention structures, and protection of river buffer zones using riparian vegetation to enhance infiltration capacity and reduce erosion.

Population Density

Population density is a key social parameter influencing flood vulnerability and flood control capacity, as it is closely associated with human activity intensity, land-use pressure, and the adaptive capacity of local communities. Areas with high population density generally experience greater exposure and sensitivity to flood hazards due to increased demand for land and infrastructure.

In the KEK Mandalika area, zones with high population density—particularly in Kuta Village and its surrounding areas—exhibit higher levels of flood vulnerability. Population growth has led to an expansion of built-up areas and increased pressure on existing drainage systems. Furthermore, community behavior related to waste management and the maintenance of drainage channels often exacerbates flood risk, especially during the rainy season when blockages reduce drainage efficiency.

To mitigate flood risk associated with high population density, government agencies and relevant institutions should focus on strengthening community capacity in environmental management and micro-drainage systems. Additional measures include reorganizing dense residential areas by integrating infiltration zones, implementing public education programs, and promoting Community-Based Flood Management (CBFM) initiatives to enhance preparedness and raise awareness of flood risks.

5. Conclusion

The rainfall parameter exhibits a highly fluctuating temporal pattern. The years 2018 and 2023 represent dry periods with the lowest annual rainfall, whereas 2019 experienced an increase from dry to moderately wet conditions with relatively uniform spatial distribution. Rainfall conditions were consistently moderately wet in 2017, 2020, and 2021, while 2022 recorded an extreme increase, reaching the wet category.

Slope analysis indicates that the study area is predominantly characterized by a score of 5, representing flat terrain (0–8%), which significantly increases the potential for flood inundation. Land cover conditions were relatively stable during 2017–2019, deteriorated in 2020, and subsequently improved from 2021 to 2023. River density is classified as very high, as indicated by the widespread dominance of scores 5 and 4, resulting in a large extent of potentially flood-prone areas.

Elevation remains temporally constant; however, low-lying areas consistently exhibit high scores (4–5), particularly in coastal zones and downstream floodplains, making these areas a priority for flood mitigation measures. Population density shows a gradual increase during 2017–2020 and 2021–2023, especially in tourism core villages, thereby amplifying social and economic risks when flooding occurs.

Land cover and slope are identified as the most dominant and representative parameters in shaping stable flood vulnerability patterns throughout the 2017–2023 period. Rainfall, elevation, and river density exhibit moderate sensitivity, while population density demonstrates the lowest sensitivity due to its strong dependence on administrative boundaries. Weighting schemes significantly influence spatial patterns, with higher weights assigned to representative parameters producing more accurate and rational flood vulnerability maps. The recommended final weights are 30% for land cover, 25% for slope, 15% for elevation, 12% for river density, 10% for rainfall, and 8% for population density.

On average, flood vulnerability zones consist of 26.51% low vulnerability, 50.66% medium vulnerability, and 22.83% high vulnerability areas. Among the analyzed parameters, those that can be directly intervened through management and policy measures include land-use planning, river network management, and population density control.

Funding: This research received no external funding.
Conflicts of Interest: The authors declare no conflict of interest.
Publisher's Note: All claims expressed in this article are solely those of the authors and do not necessarily represent those of their affiliated organizations, or those of the publisher, the editors and the reviewers.

References
References to the work should follow the 7th APA style and carefully checked for accuracy and consistency. Please ensure that every reference cited in the text is also present in the reference list and vice versa.

[1] Arfina, Paharuddin dan Sakka. 2014. Analisis Spasial untuk Menentukan Zona Risiko Bencana Banjir Bandang (Studi Kasus Kabupaten Pangkep). Prosiding Seminar Nasional Geofisika, Optimaliasasi Sains dan Aplikasinya dalam Peningkatan Daya Saing Bangsa. Makassar.
[2] Asdak, C. 2002. Hidrologi dan Pengelolaan Daerah Aliran Sungai. Gajah Mada University Press. Yogyakarta.
[3] A. Kusuma and S. Pratama, "Analisis sensitivitas pada model penentuan daerah risiko banjir menggunakan teknik pembobotan multi-kriteria," Jurnal Sistem Informasi Geografis, vol. 9, no. 1, pp. 11–25, 2023
[4] Billa, L., Shattri, M., Pradhan, B., & Yusoff, I. (2015). GIS-based multi-criteria analysis for flood vulnerability mapping. Environmental Earth Sciences, 74(6), 5057-5070.
[5] Belton, V. & Stewart, T. (2002). Multiple Criteria Decision Analysis: An Integrated Approach. Springer.
[6] Boroushaki, S., & Malczewski, J. (2008). Implementing MCDA using GIS: A case study. International Journal of Geographical Information Science, 22(1), 23-40.
[7] Budiyanto, E. (2020). Pengaruh perubahan penggunaan lahan terhadap banjir kawasan pesisir. Jurnal Geografi, 12(2), 77–84.
[8] Burrogh, P., & McDonnell, R. (2015). Principles of Geographical Information Systems. Oxford University Press
[9] Carver, S. J. (1991). Integrating multi-criteria evaluation with geographical information systems. International Journal of Geographical Information System, 5(3), 321-339. Chang, K.T. (2019) Introduction to Geographic Information System (9th ed.) McGraw Hill.
[10] Cutter, S. L., Boruff, B. J., & Shirley, W. L. (2003). Social vulnerability to environmental hazards. Social Science Quarterly, 84(2), 242–261. https://doi.org/10.1111/1540-6237.8402002
[11] Chen, Y., & Yu, J. (2018). Spatial multi-criteria decision analysis in flood risk management. Water Resources Management, 32(12), 3925-3943.
[12] Darmawan, K., dan Suprayogi, A., 2017. Analisis tingkat kerawanan banjir di kabupaten sampang menggunakan metode overlay dengan scoring berbasis sistem informasi geografis. Jurnal Geodesi Undip, Vol.6(1): 31-40.
[13] Darmawan, D 2011. Teknologi pembelajaran. Remaja Rosdakarya. Bandung.
[14] D. Santos and G. Wirawan, "Evaluasi perubahan kerentanan banjir pada kawasan ekonomi khusus melalui pemodelan spasial," Jurnal Kebencanaan Indonesia, vol. 6, no. 1, pp. 1–15, 2023
[15] Dewan, A. (2013). Floods in a Megacity: Geospatial Techniques in Assessing Hazards, Risk, and Vulnerability. Springer
[16] Dewi, 2010. Kesiapan Sumber Daya Manusia Kesehatan Dalam Penanggulangan Masalah Kesehatan Akibat Bencana Banjir di Provinsi DKI Jakarta. Fakultas Kesehatan Masyarakat. Universitas Indonesia.
[17] Ella Y. Dan Usman S. 2008. Mencerdasi Bencana. Grasindo. Jakarta.
[18] Fauzi, R., Prasetyo, H., & Lestari, D. (2023). Analisasi spasial kemampuan pengendalian banjir di Kabupaten Lombok Tengah menggunakan MADM-GIS. Jurnal Geomatika Indonesia, 7(1), 22-34.
[19] Feizizadeh, B., & Blaschke, T. (2013). GIS-multicriteria decision analysis for landslide susceptibility mapping: omCpararing three methods for the Urmia Lake basin, Iran. Natural Hazards. 65(3), 2105-2128.
[20] Hamby, D. M. (1994). A review of techniques for parameter sensitivity analysis of environmental models. Environmental Monitoring and Assessment, 32(2), 135–154.
[21] Hwang, C. L., & Yoon, K. (1981). Multiple Attribute Decision Making: Methods and Applications. Springer-Verlag, Berlin
[22] Helton, J. C. (1993). Uncertainty and sensitivity analysis techniques for use in performance assessment for radioactive waste disposal. Reliability Engineering & System Safety, 42(2–3), 327–367. https://doi.org/10.1016/0951-8320(93)90097-I
[23] Hendriana, Komang Ika; Yasa I Gede A. S; Kesiman, Made Windu A. dan Sunarya, I Made Gede. 2013. Sistem Informasi Geografis Penentuan Wilayah Rawan Banjir di Kabupaten Buleleng. Kumpulan Artikel Mahasiswa Pendidikan Teknik Informatika (KARMAPATI) Volume 2, No: 5. Bali.
[24] Heywood, I., Cornelius, S., & Carver, S. (2011). An Introduction to GeographicalInformation System (4th ed.) Person Education
[25] Hwang, C.L. & Yoon, K. (1981). Multiple Attribute Decision Making: Methods and Applications. Springer_Verlag.
[26] Indra, Rollien. 2013. Penatagunaan Lahan Berbasis Mitigasi Bencana Longsor di Hulu DAS Lesti. Skripsi. Universitas Brawijaya. Malang.
[27] I. Arsyad and M. Bakri, "Penilaian risiko banjir berbasis Multi Criteria Decision Analysis (MCDA) dan data spasial," Jurnal Pengelolaan Sumber Daya Air, vol. 12, no. 1, pp. 13–24, 2018

[28] International Strategy for Disaster Reduction (ISDR). 2005. Kerangka Kerja Aksi Hyogo 2005-2015 (membangun ketahanan bangsa dan jomunitas terhadap bencana). Ekstrasi dari laporan Akhir World Comference on Disaster Reduction.
[29] Jafrianto, A., Sekartaji, A., Natunazah, I., dan Anisa, F., 2017. Analisis Tingkat Kerawanan Banjir Di Kelurahan Wonoboyo Menggunakan Sistem Informasi Geografis.
[30] Jonkowski, P. (1995). Integrating geographical information systems and multiple criteria decision-making method. International Journal og Geographical Information Systems, 9(5), 441-465.
[31] Judy O. Waani, Rizaldy Alfan Suneth dan Tungka Aristotulus E., 2020. Respon Masyarakat di Kawasan Permukiman Padat Menurut Tingkat Kerawanan Banjir di Kecamatan Wenang Kota Manado, Jurnal Spasial Vol. 7 No 3.
[32] Jokowinarno, Dwi. 2011. Mitigasi Bencana Tsunami di Pesisir Lampung. Jurnal Rekayasa Vol. 15 No 1, April 2011. Bandar Lampung.
[33] Khalis Ilmi, M. 2021. Penentuan Indeks Penggunaan Air (IPA) Sebagai Salah Satu Indukator Hidrologi Penilaian Kesehatan Daerah Aliran Sungai (DAS) do DAS Dodokan, Pulau Lombok, Indonesia. Jurnal SIGMA. Jurnal Teknik Sipil. Prodi Teknik Sipil FATEK UMMAT, Vol. 1 No. 2 Agustus 2021, Hal.63-69
[34] K. Chandra and P. Sihombing, "Kajian perubahan tata guna lahan terhadap peningkatan kerentanan banjir berbasis GIS," Jurnal Lingkungan dan Kebencanaan, vol. 9, no. 2, pp. 77–89, 2020
[35] Kuswadi, D., Zulkarnain, I., dan Suprapto, S., 2014. Identifikasi Wilayah Rawan Banjir Kota Bandar Lampung Dengan Aplikasi Sistem Informasi Geografis (SIG). Jurnal Ilmiah Teknik Pertanian-TekTan, Vol.6(1): 22-33.
[36] Kodoatie, Robert dan Sjarif Roestam. 2010. Tata Ruang Air. Hal. 151-155. Penerbit Andi. Yogyakarta.
[37] L. Dewi and Y. Mahendra, "Pemetaan potensi banjir menggunakan Weighted Overlay pada GIS: Studi kasus kawasan pesisir selatan," Jurnal Penginderaan Jauh Indonesia, vol. 4, no. 1, pp. 55–67, 2020
[38] Longley, P.A., Goodchild, M.F., Maguire, D.J., & Rhind, D.W. (2015) Geographic Information System and Science (4th ed.) John Wiley & Sons.
[39] M. Irawan and A. Ferdian, "Pengaruh tingkat kepadatan penduduk terhadap kerentanan banjir dengan pendekatan MCDA–GIS," Jurnal Perencanaan Wilayah, vol. 18, no. 1, pp. 34–49, 2022
[40] Malczewski, J. (1999). GIS and multicriteria decision analysis. John Wiley & Sons.
[41] Munir, A. Q. (2017). Sistem Informasi Geografi Pemetaan Bencana Alam Menggunakan Google Maps. Respati, 9(26).
[42] Nugroho, A., Rahman, H., & Widodo, D. (2019). Analisis Kemampuan pengendalian banjir berbasis AHP-GIS. Jurnal Teknik Sipil dan Lingkungan, 6(2), 101-110.
[43] Novitasari, L. 2015. "Geografic Information System of Android-Base Residential Locations," in 4th International Conference on Information Technology and Engineering Application 2015 (ICBA2015). Bina Darma University. Palembang.
[44] Paimin, dkk (2009). Teknik Mitigasi Bencana Banjir dan Tanah Longsor. Balikpapan: Tropenbos International Indonesia Programme.
[45] Pangastuti, E. I., & Astutik, S. (2021). Assessment of Flood Hazard Mapping Based on AHP and GIS: Kencong District. Geosfera (example citation).
[46] P. Johan and R. Lestari, "Integrasi data DEM resolusi tinggi dan AHP untuk pemetaan zona rawan banjir," Jurnal Geospasial Nasional, vol. 3, no. 2, pp. 22–34, 2022
[47] Prahasta, E. 2001. Konsep-konsep Dasar Sistem Informasi Geografis, Informatika. Bandung.
[48] Pratama, J. D., Wulandari, A., dan Mulki, G. Z., 2020. Klasifikasi Tingkat Kerentanan Daerah Banjir di Kecamatan Putussibau Selatan Kabupaten Kapuas Hulu. JeLAST: Jurnal PWK, Laut, Sipil, Tambang, Vol.7(2).
[49] Rahmati, O. et al (2016). "Flood hazad mapping using a hybrid model of multi-criteria decision analysis and GIS." Water Resources Management, 30(9):3043-3058.
[50] Ramadona, Aditya L dan Kusnanto Hari. 2008. Open Source: GIS Aplikasi Quantum GIS untuk Sistem Informasi Lingkungan. PSLH-UGM Press. Yogyakarta.
[51] R. Aditi, H. Wijaya, and A. Prakoso, "Analisis kerentanan banjir berbasis GIS di wilayah pesisir menggunakan parameter geomorfologi," Jurnal Teknik Hidrologi, vol. 5, no. 2, pp. 45–56, 2017
[52] R. Basuki and N. Sari, "Integrasi AHP–GIS untuk pemetaan daerah rawan banjir di wilayah urban," Jurnal Geomatika, vol. 15, no. 3, pp. 101–115, 2019
[53] R. Fadli and L. Anwar, "Perbandingan model fuzzy–MCDM dan AHP–GIS untuk penilaian risiko banjir perkotaan," Jurnal Teknik Sipil Indonesia, vol. 28, no. 2, pp. 87–98, 2021
[54] R. Hidayah and D. Kusnadi, "Analisis sensitivitas parameter hidrologi pada model penilaian risiko banjir berbasis spasial," Jurnal Hidrologi Tropis, vol. 13, no. 2, pp. 120–133, 2021
[55] Rofiat Bunmi Mudashiru, Nurida Sabtu, Ismail Abustan, Waheed Balogun., 2021. Metode Pemetaan Bahaya Banjir, Elsevier. (Review Jurnal)
[56] Rosyidah, L., & Hidayat, F. (2023). Kajian risiko banjir kawasan Sirkuit Mandalika menggunakan analisis geomorfometri. Jurnal Teknik Sipil dan Lingkungan, 9(1), 47–58.
[57] Saaty, T. L. (1980). The analytic hierarchy process: Planning, priority setting, resource allocation. New York: McGraw-Hill.

[58] Saltelli, A. Chan, K., & Scott, E.M. (2000). Sensitivity Analysis. John Wiley & Sons.
[59] Saltelli, A., Ratto, M., Andres, T., Campolongo, F., Cariboni, J., Gatelli, D., & Tarantola, S. (2008). Global Sensitivity Analysis: The Primer. John Wiley & Sons.
[60] Saltelli, A., Tarantola, S., Campolongo, F., & Ratto, M. (2004). Sensitivity analysis in practice: A guide to assessing scientific models. Chichester: John Wiley & Sons.
[61] Sari, M., Yuliani, T., & Handoko, F. (2021). Evaluasi sistem drainase dan kemampuan pengendalian banjir kota Surakarta. Jurnal Rekayasa Teknik Sipil, 10(3), 45-56.
[62] Sholahuddin, M., 2015. SIG untuk memetakan daerah banjir dengan metode skoring dan pembobotan (Studi Kasus Kabupaten Jepara). Jurnal Sistem Informasi, Jurnal_14777.
[63] Smith, Keith and Petley, David N. 2009. Environmental Hazards: Assessin Risk and Reducing Disater. Fifth Edition. Routledge. New York, NT.
[64] Suhardjo, Dradjat. 2010. Upaya Menciptakan Ketahanan Hidup dalam Ancaman Bahaya Laten Bencana Alam di Purworejo. Simposium Nasional Menuju Purworejo Dinamis dan Kreatif. Yogyakarta.
[65] Sunaryo, M. T. 2001. Pengelolaan Daerah Pengaliran Sungai. Makalah Seminar Peranan Lingkungan Dalam Pengelolaan Daerah Pengaliran Sungai. BAPEDAL. Jakarta. Suripin, 2004. Sistem Drainase Perkotaan yang Berkelanjutan. Penerbit Andi. Yogyakarta.
[66] Sutanta, H., Hadi, A. S., & Suryono, D. (2021). Analisis dampak perubahan tata guna lahan terhadap limpasan permukaan di kawasan Mandalika, Lombok Tengah. Jurnal Geomatika, 27(2), 111–123.
[67] Syofyan, Irwandy; Jhonerie Rommie dan Siregar, Yusni Ikhwan. 2010. Aplikasi Sistem Informasi Geografis Dalam Penentuan Kesesuaian Kawasan Jaring Tancap dan Rumput Laut di Perairan Pulau Bunguran Kabupaten Natuna. Jurnal Perikanan dan Kelauatan 15,2 (2010) : 111-120. Riau.
[68] Turban E. 2005. Decision Support System dan Inteligent System. Andi Offset.MYogyakarta.
[69] Todingan, M. P., Sinolungan, M., Kamagi, Y. E., dan Lengkong, J., 2014. Pemetaan Daerah Rawan Longsor di Wilayah Sub DAS Tondano dengan Sistem Informasi Geografis. In COCOS Vol.4(2).
[70] Triantaphyllou, E., & Sánchez, A. (1997). A sensitivity analysis approach for some deterministic multi-criteria decision-making methods. Decision Sciences, 28(1), 151–194.
[71] Utama, Lusi dan Naumar, Afrizal. 2015. Kajian Kerentanan Kawasan Berpotensi Banjir Bandang dan Mitigasi Bencana pada Daerah Aliran Sungai (DAS) Batang Kuranji Kota Padang. Jurnal Rekayasas Sipil Vol (9) : No 1-2015 ISSN 1978-5658. Padang.
[72] Widianti, Ati. 2008. Aplikasi Manajemen Risiko Bencana Alam dalam Penataan Ruang Kabupaten Nabire. Jurnal Sains dan Teknologi Indonesia Vol. 10 1 April 2008:7
[73] Y. Mahmud and T. Wardani, "Model penilaian risiko banjir di kawasan wisata pesisir menggunakan pendekatan MCDA," Jurnal Pariwisata dan Lingkungan, vol. 7, no. 4, pp. 205–220, 2019
[74] Zhang, W., Liu, X., Yu, W., Cui, C., dan Zheng, A., 2022. Spatial-Temporal Sensitivity Analysis of Flood Control Capability in China Based on MADM-GIS Model. Entropy, Vol.24(6): 772.